

NRL Report 8049

Enhancement of Fatigue Crack Growth and Fracture Resistance in Ti-6Al-4V and Ti-6Al-6V-2Sn Through Microstructural Modification

G. R. YODER, L. A. COOLEY, AND T. W. CROOKER

*Strength of Metals Branch
Engineering Materials Division*

November 24, 1976



NAVAL RESEARCH LABORATORY
Washington, D.C.

SECURITY CLASSIFICATION OF THIS PAGE (When Data Entered)

REPORT DOCUMENTATION PAGE		READ INSTRUCTIONS BEFORE COMPLETING FORM	
1. REPORT NUMBER NRL Report 8049	2. GOVT ACCESSION NO.	3. RECIPIENT'S CATALOG NUMBER	
4. TITLE (and Subtitle) ENHANCEMENT OF FATIGUE CRACK GROWTH AND FRACTURE RESISTANCE IN Ti-6Al-4V AND Ti-6Al-6V-2Sn THROUGH MICROSTRUCTURAL MODIFICATION		5. TYPE OF REPORT & PERIOD COVERED Final report on one phase of a continuing NRL Problem	
		6. PERFORMING ORG. REPORT NUMBER	
7. AUTHOR(s) G. R. Yoder, L. A. Cooley, and T. W. Crooker		8. CONTRACT OR GRANT NUMBER(s)	
9. PERFORMING ORGANIZATION NAME AND ADDRESS Naval Research Laboratory Washington, D. C. 20375		10. PROGRAM ELEMENT, PROJECT, TASK AREA & WORK UNIT NUMBERS NRL Problems M01-24 and M01-25, RR 022-01-46	
11. CONTROLLING OFFICE NAME AND ADDRESS		12. REPORT DATE November 24, 1976	
		13. NUMBER OF PAGES 23	
14. MONITORING AGENCY NAME & ADDRESS (if different from Controlling Office)		15. SECURITY CLASS. (of this report) Unclassified	
		15a. DECLASSIFICATION/DOWNGRADING SCHEDULE	
16. DISTRIBUTION STATEMENT (of this Report) Approved for public release; distribution unlimited.			
17. DISTRIBUTION STATEMENT (of the abstract entered in Block 20, if different from Report)			
18. SUPPLEMENTARY NOTES			
19. KEY WORDS (Continue on reverse side if necessary and identify by block number) Fatigue crack propagation Microstructural modification Fracture toughness Titanium alloys Heat treatment			
20. ABSTRACT (Continue on reverse side if necessary and identify by block number) Significant enhancement of fatigue crack propagation resistance and plane-strain fracture toughness was obtained in commercial-purity Ti-6Al-4V and Ti-6Al-6V-2Sn by microstructural modification. These alloys were studied in 25.4-mm-thick plates with interstitial oxygen contents of 0.20 and 0.17 weight percent, respectively. Heat treatments were chosen to provide widely varied microstructures; they were a mill anneal, a recrystallization anneal, and a			

(Continued)

20. Continued

beta anneal. The beta anneal was found to be best for improving the crack tolerance properties in question, but it reduced yield strength 9-14% from levels associated with the original mill anneal. The recrystallization anneal significantly enhanced plane-strain fracture toughness and marginally improved fatigue crack propagation resistance with negligible loss of yield strength.

CONTENTS

INTRODUCTION	1
BACKGROUND	1
MATERIALS AND HEAT TREATMENTS	3
EXPERIMENTAL DETAILS	4
RESULTS	5
DISCUSSION.....	5
Fatigue Crack Propagation	5
Plane-Strain Fracture Toughness	11
CONCLUSIONS.....	12
ACKNOWLEDGMENTS	13
REFERENCES	13
APPENDIX A—Fatigue Crack-Growth Data for Ti-6Al-4V Alloy	15
APPENDIX B—Fatigue Crack-Growth Data for Ti-6Al-6V-2Sn Alloy	18

ENHANCEMENT OF FATIGUE CRACK GROWTH AND FRACTURE RESISTANCE IN Ti-6Al-4V AND Ti-6Al-6V-2Sn THROUGH MICROSTRUCTURAL MODIFICATION

INTRODUCTION

Ti-6Al-4V and Ti-6Al-6V-2Sn are high-strength structural alloys used in weight-critical aerospace applications. In these applications, high tensile strength must be balanced against adequate crack tolerance to achieve overall structural integrity. Though recent studies have shown that plane-strain fracture toughness K_{Ic} generally can be improved by heat treatment, there is no general agreement as to the degree of the accompanying sacrifice in strength level. It is even more disturbing to find the literature confused and contradictory with regard to the possibilities of enhancing fatigue crack propagation (FCP) resistance by microstructural alteration.

The object of the work presented here is to help resolve the issue of whether Region-2 FCP resistance and K_{Ic} can be affected significantly by microstructural control in commercial-purity Ti-6Al-4V and Ti-6Al-6V-2Sn. Region-2 FCP resistance and K_{Ic} in both Ti-6Al-4V and Ti-6Al-6V-2Sn have been investigated for microstructures associated with the mill anneal (MA), recrystallization anneal (RA), and beta anneal (BA).

BACKGROUND

Fatigue crack-growth rates (da/dN) for structural alloys are commonly analyzed as a function of the fracture mechanics stress-intensity factor range ΔK according to the power law relationship proposed by Paris and Erdogan [1]:

$$da/dN = C(\Delta K)^m. \quad (1)$$

However, a logarithmic plot of da/dN vs ΔK over the full spectrum of ΔK levels associated with the fatigue process is typically sigmoidal in form, as shown schematically in Fig. 1. Region 1 occurs at low ΔK levels ($\Delta K \lesssim 11 \text{ MPa} \cdot \text{m}^{1/2}$ for high-strength titanium alloys) and is characteristic of a threshold condition for nonpropagating cracks, whereas Region 3 occurs at high ΔK levels approaching unstable fracture. It is the behavior between the upper and lower inflection points (i.e., Region 2), which is most often approximated by Eq. (1), that will be addressed in this report. Fatigue-crack propagation behavior in this region is of prime concern to the analysis of finite-life structural fatigue.

In the case of titanium alloys, the influence of heat treatment, and the resulting microstructural modification, on Region 2 FCP behavior are not well understood [2-4]. Typically, these alloys are employed in the mill-annealed condition. However, evidence

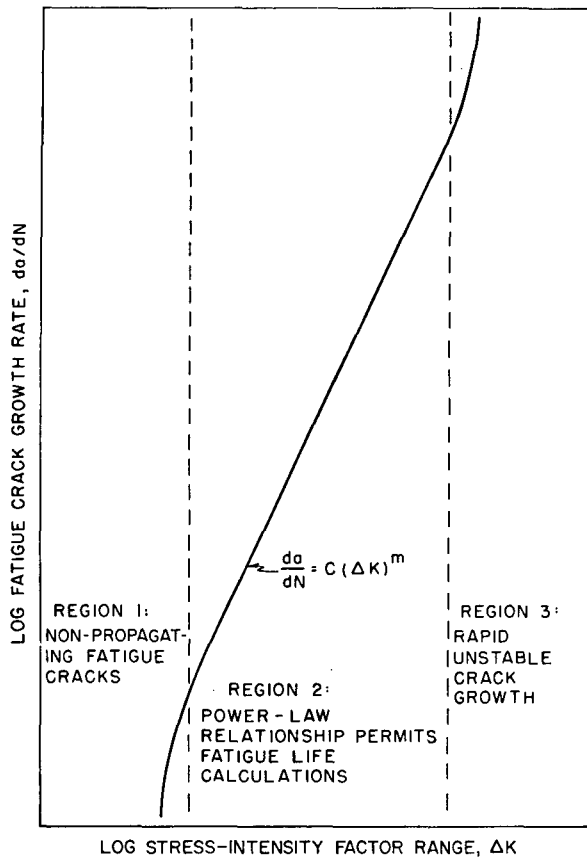


Fig. 1—Sigmoidal fatigue-crack propagation relationship

now exists to suggest that this condition may be associated with far less desirable crack tolerance properties than are achievable by other heat treatments, such as the RA and BA.

Confusion abounds as to the effects of such heat treatment/microstructural modifications on FCP resistance. Harrigan et al. [5] found with a Ti-6Al-4V alloy of commercial purity that the RA and BA offer major improvements over the MA in Regions 2 and 3. On the other hand, Irving and Beevers [6] found for a Ti-6Al-4V alloy of comparable chemistry and microstructures that FCP resistance was microstructurally insensitive in Region 2. They did, however, find substantial sensitivity to heat treatment in Region 1, as has also been observed for steel and aluminum alloys [7,8]. Microstructurally insensitive behavior was also reported by DeMay [9], who observed no difference in Region-2 FCP rates for the RA and MA in Ti-6Al-4V.

Data for the Ti-6Al-6V-2Sn system are more limited than for Ti-6Al-4V. Amateau et al. [10] reported some improvement in FCP resistance with heat treatment. However, Kondas et al. [11] and DeMay [9] found little and no beneficial effects, respectively, from the RA. Other fragments of evidence for both the 6-4 and 6-6-2 systems are summarized in Ref. 3.

Several of the investigators cited above also reported the effects of heat treatment on fracture toughness. Generally, the RA and BA were found to improve K_{Ic} ; however, the degree of improvement over mill-annealed K_{Ic} values varied considerably. Also, the reported strength levels in the heat-treated alloys varied widely. Generally, some loss of yield strength was associated with the RA and BA, but reported values of yield strength covered a wide range. For instance, in the case of commercial-purity Ti-6Al-4V, such values ranged from about 758 to 1034 MPa for beta-annealed microstructures.

MATERIALS AND HEAT TREATMENTS

The two alloys studied were in the form of 25.4-mm-thick rolled plate. Chemical analyses of both alloys appear in Table 1. Procedures followed in the three heat treatments studied are given in Table 2. Measurements of the resulting mechanical properties for the six combinations of alloy and heat treatment are tabulated in Table 3.

Table 1—Chemical Analyses (wt %)

Material	O	Al	V	Fe	Sn	Cu	N	C	H
Ti-6Al-4V	0.20	6.7	4.3	0.10	—	—	0.011	0.03	0.0060
Ti-6Al-6V-2Sn	0.17	5.5	5.3	0.57	2.3	0.62	0.012	0.03	0.0034

Table 2—Heat Treatments

Material and Heat Treatment	Specifications	References
Ti-6Al-4V		
Mill Anneal (MA)	788°C, 1 h/AC (as received)	—
Recrystallization Anneal (RA)	954°C, 4 h/HC @ 180°C/h to 760°C/HC @ 370°C/h to 482°C/AC	[5,12]
Beta Anneal (BA)	1038°C, 0.5 h/HC to RT + 732°C, 2 h/HC	[5]
Ti-6Al-6V-2Sn		
Mill Anneal (MA)	732°C, 1 h/HC	[11]
Recrystallization Anneal (RA)	893°C, 4 h/HC @ 265°C/h to 760°C, HC @ 370°C/h to 538°C/AC	[11]
Beta Anneal (BA)	1004°C, 0.5 h/HC to RT + 677°C, 2 h/HC	—

Abbreviations: HC = helium purge in vacuum furnace at a rate equivalent to air cooling, unless otherwise specified

AC = air cool

RT = room temperature

Table 3—Mechanical Properties

Material and Heat Treatment	Fracture Toughness K_{Ic} (MPa · m ^{1/2})	0.2% Yield Strength σ_{ys} (MPa)	Tensile Strength σ_{uts} (MPa)	Young's Modulus E(GPa)	Strain Hardening Exponent [*] n	Percent Reduction in Area	Percent Elongation (51 mm G.L.)
Ti-6Al-4V							
MA	40 [†] , 42 [‡]	1007	1034	130	0.021	29	14
RA	76	931	1007	130	0.041	26	15
BA	87	869	958	117	0.044	16	11
Ti-6Al-6V-2Sn							
MA	47	1043	1105	118	0.033	27	16
RA	70	1034	1109	117	0.036	31	16
BA	82	954	1056	114	0.048	27	16

*Computed according to the method of Rowe [13].

†Marginally invalid [14], as K_I (max) during precracking exceeded 60% of K_{Ic} by ≈ 3 MPa · m^{1/2}.

‡Valid determination (three-point bend bar) from earlier work [15].

EXPERIMENTAL DETAILS

Determinations of FCP rate and K_{Ic} were made from compact tension specimens of 25.4-mm thickness, with the crack propagating in the TL orientation [16]. The specimen geometry, depicted in Fig. 2, was of the WOL type with a half-height to width (h/W) ratio of 0.486. Stress-intensity factor calculations were made using the expression [17]

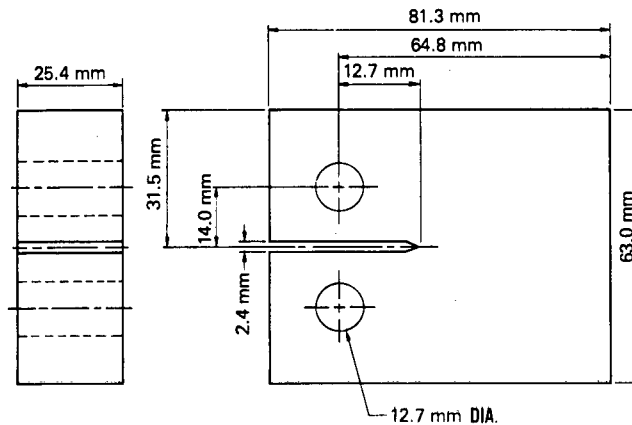


Fig. 2—Geometry of WOL type compact tension specimen

$$K_{Ic} = \frac{P\sqrt{a}}{BW} \left[30.96 - 195.8 \left(\frac{a}{W} \right) + 730.6 \left(\frac{a}{W} \right)^2 - 1186.3 \left(\frac{a}{W} \right)^3 + 754.6 \left(\frac{a}{W} \right)^4 \right], \quad (2)$$

where a = crack length, W = specimen width (64.8 mm), B = thickness (25.4 mm), and P = applied load. Specimens were loaded in ambient laboratory air. For each material and heat treatment, duplicate specimens were subjected to cyclic tension-to-tension loading with a haversine waveform, a frequency of 5 Hz, and a load ratio of $R = P_{\min}/P_{\max} = 0.1$. The amplitude of loading, while maintained constant throughout the FCP test of each specimen, was different for each of the paired specimens so that da/dN could be generated over different yet overlapping ranges of ΔK ($15 \lesssim \Delta K \lesssim 55 \text{ MPa} \cdot \text{m}^{1/2}$). With the first specimen, FCP data were obtained in the range of $0.26 \lesssim a/W \lesssim 0.53$, after which the specimen was subjected to a determination of K_{Ic} [14]. With the second specimen, cycled at the higher loading amplitude, FCP data were obtained over the range of $0.26 \lesssim a/W \lesssim 0.62$. Measurements of crack length were made at $15\times$ using a Gaertner traveling microscope.

Tensile properties were determined from standard 12.8-mm-diameter specimens with a 50.8-mm gage length.

RESULTS

The three microstructures of the Ti-6Al-4V alloy and the respective plots of FCP resistance are shown in Fig. 3, which is a logarithmic plot of da/dN vs ΔK . (These data are tabulated in Appendix A.) Parallel results for the Ti-6Al-6V-2Sn alloy are shown in Fig. 4. (These data are tabulated in Appendix B.) A summary plot of da/dN -vs- ΔK trend lines for each of the six cases studied is shown in Fig. 5.

The K_{Ic} results are plotted in Figs. 6 and 7, which are Ratio Analysis Diagram (RAD) formats of fracture toughness vs yield strength (σ_{ys}) for the generic family of high-strength titanium alloys [18]. The RAD is a cumulative summary plot showing the trend lines for maximum and minimum levels of fracture toughness measured in this family of alloys over a broad range of yield strengths. The $K_{Ic}/\sigma_{ys} = 0.63$ ratio line denotes the ASTM-defined limit for plane-strain fracture measurements [14]. Below this ratio line valid K_{Ic} values can be obtained, and above this line increasing amounts of plasticity require the use of other test methods, such as the J-integral procedure [19], for meaningful quantitative measurements of toughness. All of the data plotted in Figs. 6 and 7 are valid K_{Ic} determinations per ASTM E399-74 [14].

DISCUSSION

Fatigue Crack Propagation

For Ti-6Al-4V, the da/dN -vs- ΔK curves in Fig. 3 are distinctly ordered with respect to heat treatment. The most rapid crack-growth rates were observed in the case of the

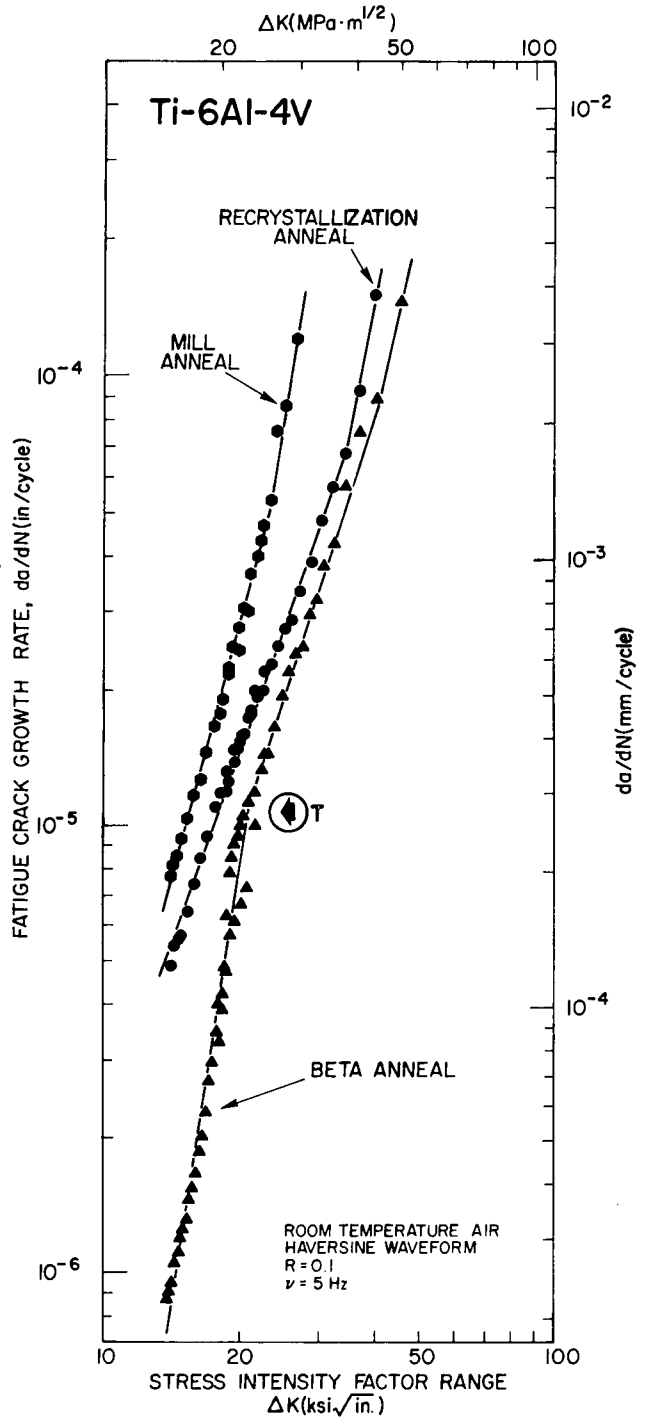
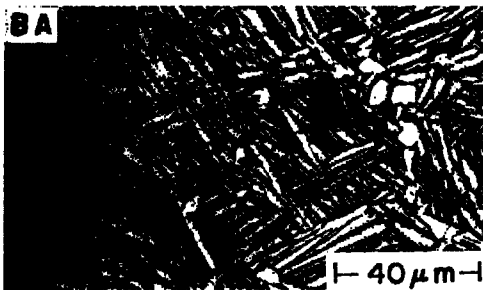
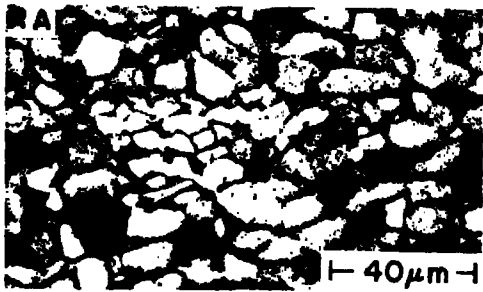
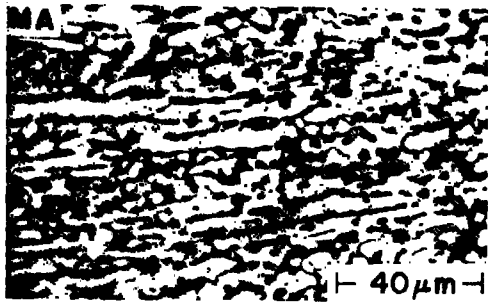


Fig. 3—Microstructures and fatigue crack-growth rates of Ti-6Al-4V for the mill anneal (MA), recrystallization anneal (RA), and beta anneal (BA)

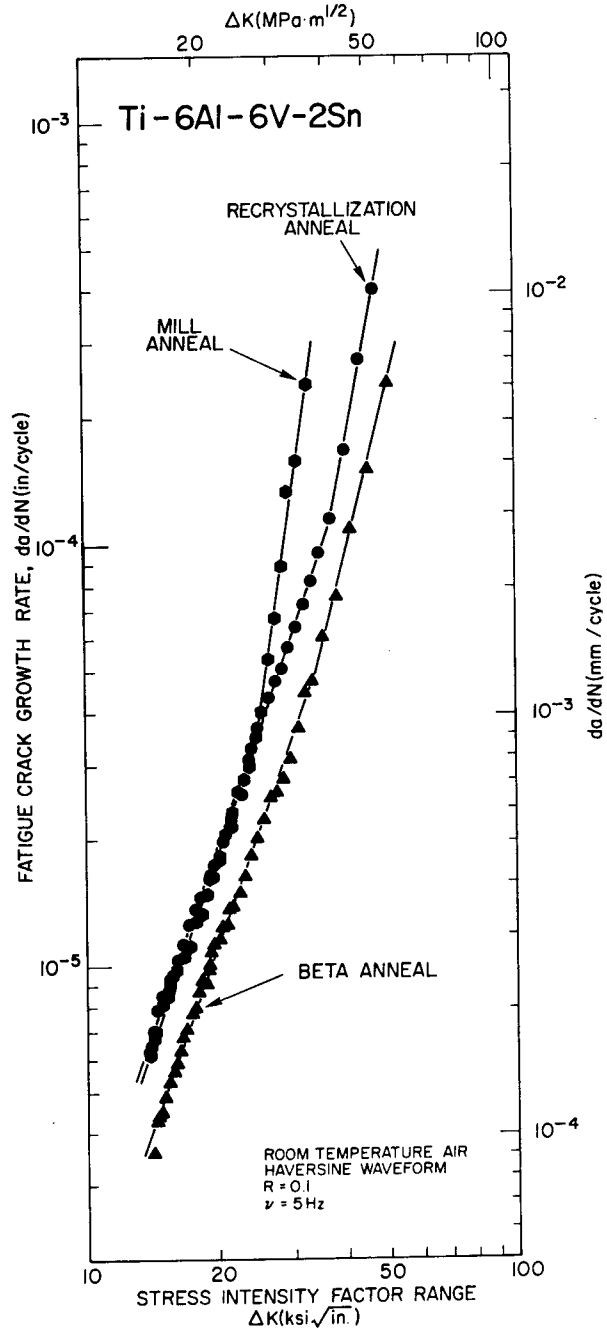
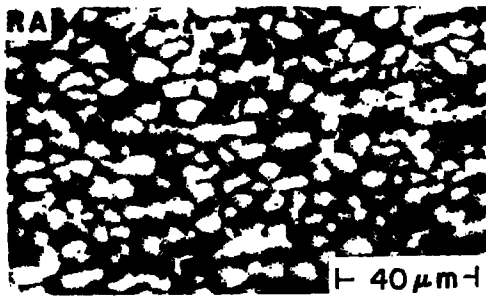
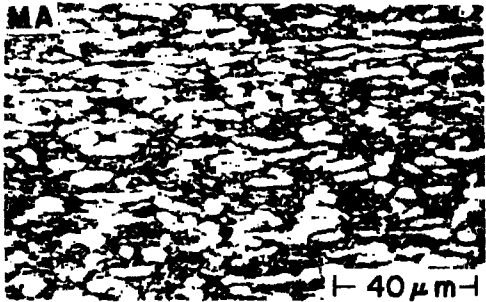


Fig. 4—Microstructures and fatigue crack-growth rates of Ti-6Al-6V-2Sn for the mill anneal (MA), recrystallization anneal (RA), and beta anneal (BA)

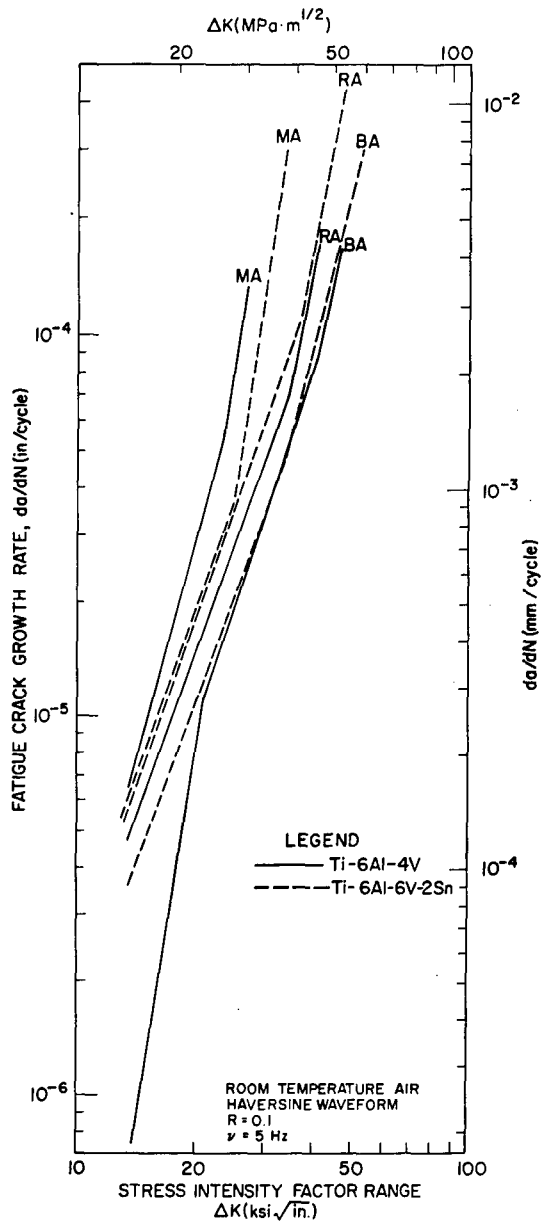


Fig. 5—Comparison of fatigue crack-growth rates in Ti-6Al-4V and Ti-6Al-6V-2Sn for the mill anneal (MA), recrystallization anneal (RA), and beta anneal (BA)

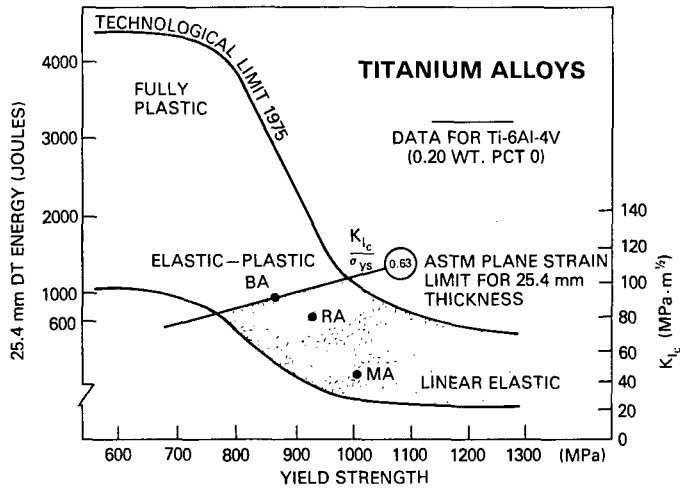


Fig. 6—Influence of heat treatment on fracture toughness and strength level of Ti-6Al-4V

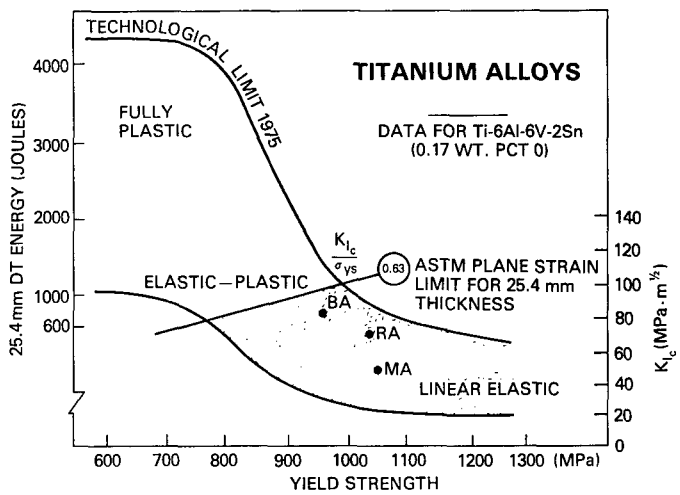


Fig. 7—Influence of heat treatment on fracture toughness and strength level of Ti-6Al-6V-2Sn

MA, and the slowest were observed for the BA; the RA provided behavior between these extremes. Overall, crack-growth rates were observed to vary by as much as an order of magnitude in response to heat treatment.

The maximum degree of beneficial response occurred with the BA at lower ΔK levels ($15 < \Delta K < 23 \text{ MPa} \cdot \text{m}^{1/2}$), below a transition point, denoted T in Fig. 3. Below T, fatigue-crack propagation was characterized by macroscopic crack-front bifurcation, as illustrated in Fig. 8. Microscopically, this mode of crack growth has been observed to occur as microstructurally sensitive cracking along crystallographic planes and has been

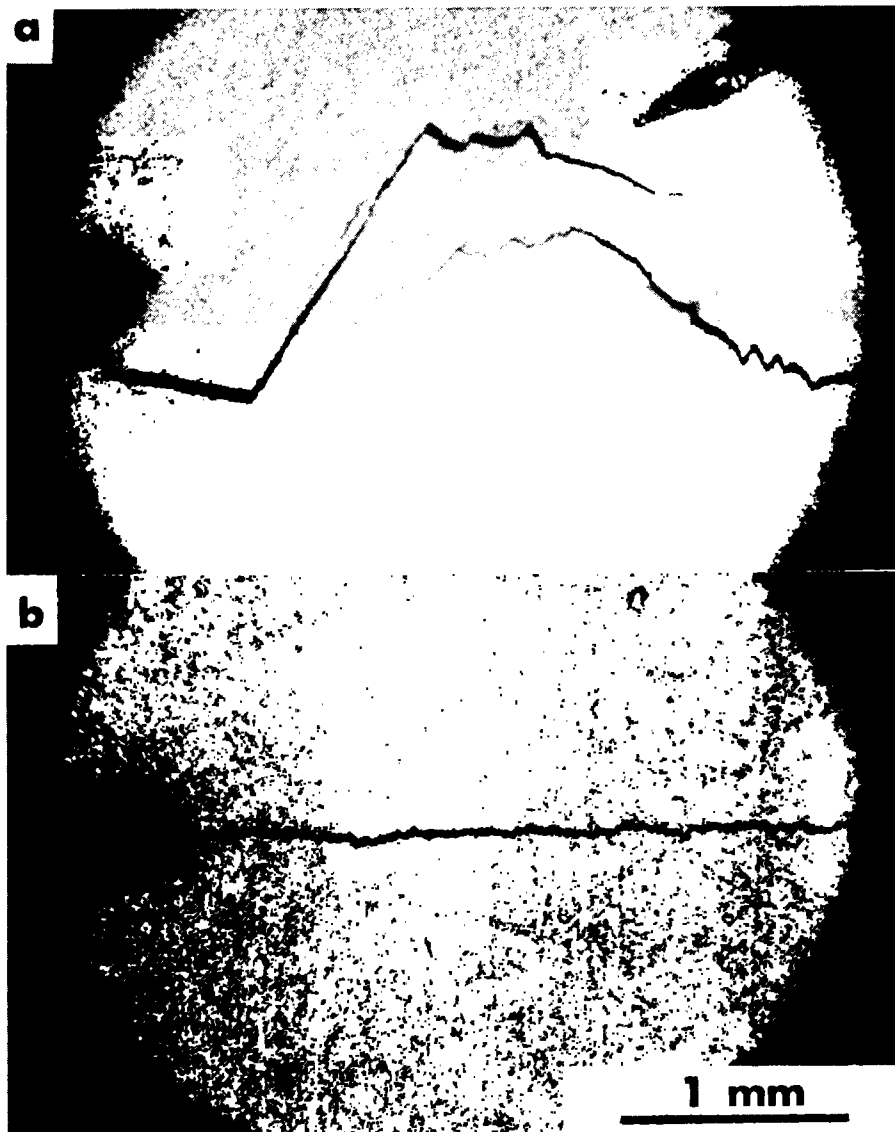


Fig. 8—(a) Crack bifurcation in the fatigue crack growth of a beta-annealed Ti-6Al-4V alloy; (b) normal, nonbifurcated Mode I fatigue crack growth in a mill-annealed Ti-6Al-6V-2Sn alloy

analyzed in detail in a separate report [20]. The net effect of crack bifurcation is to disperse the strain-field energy of the macroscopic crack among multiple crack tips and increase the surface area generated during crack propagation, thus significantly decreasing crack-growth rates. Among the six combinations of alloy and heat treatment studied, only in the case of the BA in the Ti-6Al-4V alloy did this bifurcation appear; the macroscopic effect of this microscopic difference in behavior is quite apparent on the da/dN -vs- ΔK summary plot of Fig. 5.

Significant enhancement of FCP resistance in high-strength titanium alloys depends largely on microstructurally sensitive crack propagation such as is seen here for the BA in the Ti-6Al-4V. Further fundamental investigation is required to explain the exact metallurgical conditions that give rise to it. However, these observations do lend support to the work reported by Harrigan et al., and serve to focus further attention on the BA heat treatment as a means of significantly enhancing the FCP resistance of commercial-purity Ti-6Al-4V alloys.

For the three microstructures of the Ti-6Al-6V-2Sn alloy (Fig. 4), a similar but less pronounced ordering of the da/dN -vs- ΔK curves with heat treatment was observed. The RA produced little effect on crack-growth rates except at higher ΔK levels approaching fracture. This is in general agreement with the results of Kondas et al. [11] and DeMay [9] on commercial-purity Ti-6Al-6V-2Sn alloys. The BA resulted in modest improvements in FCP resistance at all ΔK levels studied, with da/dN values reduced by approximately a factor of two for the BA. No significant evidence of crack-front bifurcation was observed in the Ti-6Al-6V-2Sn BA material. However, the upper branch of the da/dN -vs- ΔK curve above T for the BA in Ti-6Al-4V and the curve for the BA in Ti-6Al-6V-2Sn virtually overlap, as shown in Fig. 5.

It might be further observed that the ordering of fatigue crack-growth rates as a function of heat treatment in Figs. 3 and 4 appears to correlate with strength level and the inverse of the strain-hardening exponents listed in Table 3. Such a relation is consistent with some models of FCP resistance, although it is uncertain that any correlation with hardening exponents should be based on monotonic rather than cyclic strain-hardening (or softening) behavior.

Inasmuch as several investigators have reported that FCP rates for different materials can be normalized with respect to Young's modulus (E), it is pertinent to note that the da/dN -vs- ΔK curves of Figs. 3 and 4 cannot be normalized on this basis. If such a normalization were undertaken using the values of E in Table 3, the curves would actually diverge from their present positions.

Plane-Strain Fracture Toughness

A similar ordering of the K_{Ic} and σ_{ys} results with heat treatment is apparent in the data plotted in Figs. 6 and 7. As with the FCP data, the MA is associated with the lowest values of K_{Ic} for each alloy. The maximum improvement here is also obtained via the BA, with the RA producing intermediate results. As given in the tabulated values of K_{Ic} (Table 3), the BA serves to roughly double the fracture toughness of both alloys from levels associated with the MA. Also, in both alloys the RA imparts substantial benefits to K_{Ic} values.

However, as also illustrated in Figs. 6 and 7, the RA and BA are accompanied by a loss of yield strength, most pronounced for the BA. The BA causes reductions in yield strength of 9% and 14% in Ti-6Al-6V-2Sn and Ti-6Al-4V, respectively, from levels associated with the MA. Nevertheless, it is encouraging that for both alloys the RA substantially enhances K_{Ic} values with minor loss of yield strength. This agrees with the findings of Kondas et al. [11].

The tangible benefit of processing structural alloys to achieve higher fracture toughness is the ability of the metals to tolerate larger critical crack sizes without fracturing unstably. As presented in Table 4, critical crack sizes for fracture in these materials are substantially increased by heat treatment. In both alloys, the critical crack sizes for the MA are barely within the detectable range for even sophisticated nondestructive inspection procedures. By heat treatment, these critical crack sizes can be increased to a size at which detection before failure becomes much more probable.

CONCLUSIONS

The results obtained from this investigation have shown that the FCP resistance and plane-strain fracture toughness of commercial-purity Ti-6Al-4V and Ti-6Al-6V-2Sn alloys are significantly enhanced through recrystallization and beta anneals, as compared to the original mill-annealed condition. Specific findings are as follows:

The maximum degree of improvement in overall crack tolerance was achieved with the beta anneal. Fatigue crack-growth rates were reduced by as much as an order of magnitude in the Ti-6Al-4V, and plane-strain fracture toughness was approximately doubled in both alloys by beta annealing originally mill-annealed materials.

The penalty for achieving these marked improvements in crack tolerance was loss of yield strength, which ranged from 9% in Ti-6Al-6V-2Sn to 14% in Ti-6Al-4V.

Table 4—Critical Crack Depths
(Long, Shallow Surface Cracks)

Alloys and Heat Treatment	a (mm) $\sigma = 0.5 \sigma_{ys}$	a (mm) $\sigma = \sigma_{ys}$
Ti-6Al-4V		
MA	1.9	0.4
RA	7.5	1.6
BA	11.2	2.4
Ti-6Al-6V-2Sn		
MA	2.3	0.5
RA	5.1	1.1
BA	8.1	1.8

NRL REPORT 8049

For both alloys, the recrystallization anneal resulted in marginal to negligible reductions in fatigue crack-growth rates but substantially improved plane-strain fracture toughness with small loss of yield strength.

The most significant reductions in fatigue crack-growth rates (of approximately an order of magnitude in beta-annealed Ti-6Al-4V) were associated with microstructurally sensitive crack bifurcation. However, this phenomenon and its concomitant benefits were not observed in the beta-annealed Ti-6Al-6V-2Sn. The metallurgical conditions that give rise to this highly beneficial fatigue-crack propagation mechanism in high-strength titanium alloys are not yet fully understood.

ACKNOWLEDGMENTS

The authors are indebted to M. L. Cigledy, G. W. Jackson, C. R. Forsht, and T. R. Harrison for assistance with the experimental phases of this study. This work was supported by the Office of Naval Research.

REFERENCES

1. P. Paris and F. Erdogan, "A Critical Analysis of Crack Propagation Laws," *Trans. ASME, J. Basic Eng.* (Ser. D) 85, 528 (1963).
2. J. C. Chesnutt, C. G. Rhodes, and J. C. Williams, "The Relationship Between Mechanical Properties, Microstructure and Fracture Topography in $\alpha + \beta$ Titanium Alloys," in *Fractography—Microscopic Cracking Processes*, ASTM STP 600, American Society for Testing and Materials, Philadelphia, Pa., 1976, pp. 99-138.
3. A. Tobin, "The Role of Microstructure in Determining Fracture Toughness and Fatigue Properties of High Strength Titanium Alloys," Tech. Rep. RE-485, Grumman Aerospace Corporation, Bethpage, N.Y., Aug. 1974.
4. F. A. Crossley and R. E. Lewis, "Correlation of Microstructures with Fracture Toughness Properties in Metals," Lockheed Missiles and Space Company, Inc., Final Report on NASC Contract N00019-72-C-0545, Sept. 1973, available from NTIS, Springfield, Va., AD 772-103.
5. M. J. Harrigan, M. P. Kaplan, and A. W. Sommer, "Effect of Chemistry and Heat Treatment on the Fracture Properties of Ti-6Al-4V Alloy," in *Fracture Prevention and Control*, D. W. Hoepfner, ed. (Vol. 3 in the ASM Materials/Metalworking Technology Series), American Society for Metals, Metals Park, Ohio, 1974, pp. 225-254.
6. P. E. Irving and C. J. Beevers, "Microstructural Influences on Fatigue Crack Growth in Ti-6Al-4V," *Mater. Sci. Eng.* 14, 229 (1974).
7. C. J. Beevers, R. J. Cooke, J. F. Knott and R. O. Ritchie, "Some Considerations of the Influence of Sub-Critical Cleavage Growth During Fatigue-Crack Propagation in Steels," *Metal Sci.* 9, 119 (1975).
8. G. G. Garrett and J. F. Knott, "On the Influence of Fracture Mechanisms on Fatigue Crack Propagation in Aluminum Alloys," *Met. Trans.* 6A, 1663 (1975).

YODER, COOLEY, AND CROOKER

9. S. DeMay, "Improved Fracture Toughness of Titanium," Grumman Aerospace Corporation, Bethpage, N.Y., final report on NADC Contract N62269-73-C-0127, June 1973, available from NTIS, Springfield, Va., AD 778-652.
10. M. F. Amateau, W. D. Hanna, and E. G. Kendall, "The Effect of Microstructure on Fatigue Crack Propagation in Ti-6Al-6V-2Sn Alloy," in *Mechanical Behavior, Proceedings of the International Conference on Mechanical Behavior of Materials*; Vol. 2, The Society of Material Science, Japan, 1972, p. 77.
11. K. R. Kondas, T. W. Crooker, and C. M. Gilmore, "Cyclic-Crack-Growth and Fracture Resistance of Ti-6Al-6V-2Sn as Influenced by Recrystallization Anneal and Interstitial Oxygen Content," *Eng. Fracture Mech.* **7**, 641-647 (1975).
12. A. W. Sommer, "Materials Technology and the B-1," Report NA-72-841, North American Rockwell, Los Angeles Division, Oct. 13, 1972.
13. G. H. Rowe, "Correlation of High-Cycle Fatigue Strength with True Stress-True Strain Behavior," *J. Mater.* **1**(3), 689 (1966).
14. "Standard Method of Test for Plane-Strain Fracture Toughness of Metallic Materials," E399-74, in *1975 Annual Book of ASTM Standards*, Part 10, p. 561, American Society for Testing and Materials, Philadelphia, Pa., 1975.
15. G. R. Yoder, unpublished research.
16. R. J. Goode, "Identification of Fracture Plane Orientation," *Mater. Res. Stand.* **12**(9), 31 (Sept. 1972).
17. W. G. Clark, Jr., and S. J. Hudak, Jr., "Variability in Fatigue Crack Growth Rate Testing," *J. Testing Evaluation* **3**(6), 454 (1975).
18. R. W. Judy and R. J. Goode, "Prevention and Control of Subcritical Crack Growth in High-Strength Metals," NRL Report 7780, Aug. 2, 1974.
19. G. R. Yoder and C. A. Griffis, "Application of the J-Integral to the Initiation of Crack Extension in a Titanium 6Al-4V Alloy," in *Mechanics of Crack Growth*, ASTM STP 590, American Society for Testing and Materials, Philadelphia, Pa., 1976, pp. 61-81.
20. G. R. Yoder, L. A. Cooley, and T. W. Crooker, "A Micromechanistic Interpretation of Cyclic Crack Growth Behavior in a Beta-Annealed Ti-6Al-4V Alloy," NRL Report 8048, November 24, 1976.

Appendix A

FATIGUE CRACK-GROWTH DATA FOR Ti-6Al-4V ALLOY

This appendix contains a tabulation of the fatigue crack-growth rate (da/dN) vs stress-intensity factor range (ΔK) data plotted in Fig. 3 for the recrystallization anneal (RA), beta anneal (BA), and mill anneal (MA).

MILL ANNEAL

Specimen No. R23C-1D	
ΔK (MPa · m ^{1/2})	da/dN (mm/cycle)
15.3	1.75×10^{-4}
15.5	1.95
15.8	2.07
16.0	2.16
16.4	2.36
16.9	2.62
17.4	2.95
18.0	3.23
18.6	3.68
19.3	4.24
20.0	4.52
20.9	5.54
22.0	6.22
23.2	7.62
24.5	1.13×10^{-3}

Specimen No. R23C-2D	
ΔK (MPa · m ^{1/2})	da/dN (mm/cycle)
20.2	4.83×10^{-4}
20.6	5.64
21.2	6.35
21.9	7.01
22.6	7.82
23.3	9.25
24.1	1.02×10^{-3}
25.0	1.20
25.8	1.35
26.7	1.92
27.9	2.18
29.4	3.05

BETA ANNEAL

Specimen No. R23C-3D	
ΔK (MPa · m ^{1/2})	da/dN (mm/cycle)
15.2	2.23 × 10 ⁻⁵
15.3	2.29
15.4	2.31
15.6	2.42
15.8	2.67
16.0	2.82
16.3	3.02
16.5	3.18
16.8	3.33
17.0	3.68
17.3	3.91
17.6	4.24
17.9	4.72
18.2	5.08
18.5	5.82
18.9	6.78
19.2	7.52
19.5	8.84
19.9	1.02 × 10 ⁻⁴
20.2	1.07
20.5	1.20
20.9	1.45
21.5	1.56
22.2	1.69
23.0	1.85
23.9	2.54
24.8	3.68

Specimen No. R23C-7D	
ΔK (MPa · m ^{1/2})	da/dN (mm/cycle)
19.9	8.33 × 10 ⁻⁵
20.1	9.86
20.4	1.22 × 10 ⁻⁴
20.6	1.61
20.9	1.99
21.2	2.16
21.5	2.31
21.8	2.42
22.2	2.54
22.5	2.67
23.1	2.87
23.9	3.00
24.7	3.38
25.5	3.68
26.4	4.24
27.4	4.95
28.3	5.64
29.3	6.15
30.4	6.35
31.5	7.52
32.7	8.13
34.0	9.68
35.8	1.09 × 10 ⁻³
38.1	1.45
40.9	1.91
44.8	2.26
50.4	2.65

RECRYSTALLIZATION ANNEAL

Specimen No. R23C-4D	
ΔK (MPa · m ^{1/2})	da/dN (mm/cycle)
15.1	9.6×10^{-5}
15.3	1.1×10^{-4}
15.5	1.2
15.7	1.4
16.0	1.4
16.4	1.4
16.9	1.6
17.4	1.9
18.0	2.2
18.6	2.4
19.3	2.8
20.0	3.0
20.7	3.4
21.4	3.6
22.2	4.1
23.0	4.4
23.8	5.1
24.8	5.6

Specimen No. R23C-5D	
ΔK (MPa · m ^{1/2})	da/dN (mm/cycle)
20.3	2.7×10^{-4}
20.5	3.0
20.8	3.2
21.1	3.4
21.4	3.5
21.7	3.8
22.1	3.9
22.6	4.1
23.4	4.5
24.2	5.0
25.0	5.1
25.9	5.8
26.8	6.3
27.7	7.0
28.7	7.3
30.0	8.4
31.7	9.8
33.5	1.2×10^{-3}
35.6	1.4
38.0	1.7
40.7	2.3
44.0	3.8

Appendix B

FATIGUE CRACK-GROWTH DATA FOR Ti-6Al-6V-2Sn ALLOY

This appendix contains a tabulation of the fatigue crack-growth rate (da/dN) vs stress-intensity factor range (ΔK) data plotted in Fig. 4 for the recrystallization anneal (RA), beta anneal (BA), and mill anneal (MA).

MILL ANNEAL

Specimen No. R29-1D		Specimen No. R29-2D	
ΔK (MPa · m ^{1/2})	da/dN (mm/cycle)	ΔK (MPa · m ^{1/2})	da/dN (mm/cycle)
15.4	1.56×10^{-4}	20.8	3.8×10^{-4}
15.6	1.73	21.1	4.1
15.8	1.78	21.6	4.1
16.0	1.81	22.2	4.5
16.3	2.07	22.9	5.2
16.5	2.08	23.7	5.6
16.8	2.16	24.5	6.6
17.0	2.31	25.4	7.0
17.3	2.41	26.3	7.5
17.8	2.49	27.2	8.8
18.4	2.67	28.2	1.0×10^{-3}
19.0	2.82	29.2	1.4
19.7	3.23	30.2	1.7
20.3	3.38	31.3	2.2
21.1	3.76	32.5	3.4
22.2	4.62	34.2	4.0
23.8	5.87	36.3	6.1

RECRYSTALLIZATION ANNEAL

Specimen No. R29-7D	
ΔK (MPa · m ^{1/2})	da/dN (mm/cycle)
14.9	1.4×10^{-4}
15.1	1.5
15.2	1.6
15.4	1.7
15.6	1.8
15.9	2.0
16.1	2.0
16.4	2.2
16.6	2.2
17.0	2.4
17.6	2.6
18.2	2.9
18.8	3.2
19.5	3.4
20.2	3.7
20.9	4.1
21.6	4.4
22.6	5.0
23.9	5.4
25.3	6.5

Specimen No. R29-8D	
ΔK (MPa · m ^{1/2})	da/dN (mm/cycle)
26.1	7.8×10^{-4}
26.6	8.3
27.3	9.3
28.2	1.0×10^{-3}
29.3	1.1
30.3	1.2
31.4	1.3
32.6	1.4
33.9	1.6
35.3	1.8
36.8	2.1
38.5	2.4
40.8	2.9
44.1	4.2
48.0	6.9
52.0	1.0×10^{-2}

YODER, COOLEY, AND CROOKER

BETA ANNEAL

Specimen No. R29-4D	
ΔK (MPa · m ^{1/2})	da/dN (mm/cycle)
15.8	8.9 × 10 ⁻⁵
16.0	9.2
16.4	9.8
16.6	1.0 × 10 ⁻⁴
16.8	1.1
17.1	1.1
17.4	1.2
17.7	1.4
18.0	1.4
18.3	1.5
18.8	1.5
19.4	1.6
20.1	1.8
20.8	2.0
21.6	2.3
22.4	2.4
23.2	2.6
24.1	2.8
25.0	3.1
26.0	3.6

Specimen No. R29-5D	
ΔK (MPa · m ^{1/2})	da/dN (mm/cycle)
20.7	2.31 × 10 ⁻⁴
21.0	2.48
21.1	2.54
21.8	2.90
22.4	2.95
23.2	3.18
24.0	3.51
24.8	3.81
25.7	4.14
26.6	4.62
27.5	5.08
28.5	5.64
29.5	6.35
30.6	6.55
31.7	7.01
32.9	7.82
34.2	9.25
35.6	1.13 × 10 ⁻³
37.1	1.20
39.3	1.52
42.3	1.91
45.9	2.77
50.2	3.81
55.5	6.10